

# Photophysics of Bifunctional Ru(II) Complexes Bearing an Aminoquinoline Organic Unit. Potential New Photoprobes and Photoreagents of DNA

André Del Guerzo and Andrée Kirsch-De Mesmaeker<sup>\*,†</sup>

Université Libre de Bruxelles, Chimie Organique Physique, CP 160/08 50 avenue F. D. Roosevelt, 1050 Bruxelles, Belgium

Martine Demeunynck and Jean Lhomme

LEDSS, Université Joseph Fourier, BP 53X-38041, Grenoble CEDEX, France

Received: April 14, 1997; In Final Form: June 11, 1997<sup>®</sup>

[Ru(BPY)<sub>2</sub>POQ–Nmet]<sup>2+</sup> and [Ru(TAP)<sub>2</sub>POQ–Nmet]<sup>2+</sup> (**1** and **3**) are bifunctional complexes composed of a metallic unit linked by a flexible chain to an organic unit. They have been prepared as photoprobes or photoreagents of DNA. In this work, the spectroscopic properties of these bifunctional complexes in the absence of DNA are compared with those of the monofunctional analogues [Ru(BPY)<sub>2</sub>Phen]<sup>2+</sup>, [Ru(BPY)<sub>2</sub>acPhen]<sup>2+</sup>, [Ru(TAP)<sub>2</sub>Phen]<sup>2+</sup>, and [Ru(TAP)<sub>2</sub>acPhen]<sup>2+</sup> (**2** and **4**). The electrospray mass spectrometry and absorption data show that the quinoline moiety exists in the protonated and nonprotonated form. Although the bifunctional complex containing 2,2'-bipyridine (BPY) ligands exhibits photophysical properties similar to those of the monofunctional compounds, the bifunctional complex with 1,4,5,8-tetraazaphenanthrene (TAP) ligands behaves quite differently. It has weaker relative emission quantum yields and shorter luminescence lifetimes than the monofunctional TAP analogue when the quinoline unit is nonprotonated. This indicates an efficient intramolecular quenching of the <sup>3</sup>MLCT (metal to ligand charge transfer) excited state of the TAP metallic moiety. When the organic unit is protonated, there is no internal quenching. In organic solvent, the nonquenched excited metallic unit (bearing a protonated quinoline) and the quenched one (bearing a nonprotonated organic unit) are in slow equilibrium as compared to the lifetime of the two emitters. In aqueous solution this equilibrium is faster and is catalysed by the presence of phosphate buffer. Flash photolysis experiments suggest that the intramolecular quenching process originates from a photoinduced electron transfer from the nonprotonated quinoline to the excited Ru(TAP)<sub>2</sub><sup>2+</sup> moiety.

## Introduction

Ru(II) polypyridyl complexes have been extensively studied as photosensitizers of redox reactions.<sup>1,2</sup> For many years, the remarkable properties of these compounds have been applied in several areas: solar energy conversion<sup>3–5</sup> and storage, in photoelectrochemical cells,<sup>3,6,7</sup> and as photosensitizing building blocks in supramolecular antenna systems for charge separation<sup>8</sup> and for energy transfer. More recently, because of their attractive luminescent properties which are extremely sensitive to the microenvironment, Ru(II) complexes have also been used as photoprobes of DNA structures and conformations.<sup>9–13</sup>

In our laboratory, some of these complexes have been applied as photoreagents with DNA.<sup>14–18</sup> The complexes with TAP (TAP = 1,4,5,8-tetraazaphenanthrene) and HAT (HAT = 1,4,5,8,9,12-hexaazatriphenylene) ligands are very oxidizing in their excited <sup>3</sup>MLCT (metal to ligand charge transfer) state<sup>19–21</sup> so that they can abstract an electron from a guanine base of DNA (the most easily oxidizable base among the four nucleotide bases).<sup>14,22</sup> This primary process induces DNA cleavage<sup>14,16,23</sup> and the formation of an adduct of the complex with DNA.<sup>14,18,24</sup> These properties can thus be exploited in order to mimic endonuclease activity.<sup>25,26</sup> However, an important drawback of these photooxidizing TAP and HAT complexes is their low affinity for DNA.<sup>23,27</sup> One of the strategies which we have adopted to enhance their binding affinity for nucleic acids is

the design of bifunctional complexes composed of two units connected by an aliphatic chain (**1**, **3**, Figure 1), where each unit interacts according to its own mode with DNA. An initial bifunctional complex had already been studied with DNA in our laboratory.<sup>28</sup> However, its photophysical behavior in the absence and presence of DNA was not fully understood. Therefore we have initiated more thorough studies with other bifunctional complexes containing not only TAP but also 2,2'-bipyridine (BPY) ligands. In the present work, the photophysics and complete kinetic study of different relaxation pathways for the excited [Ru(TAP)<sub>2</sub>POQ–Nmet]<sup>2+</sup> (Figure 1) and for the corresponding BPY derivatives are examined in the absence of DNA. An aminoquinoline unit<sup>29,30</sup> with a methyl group on the amine has been chosen because the resulting complex is more easily prepared and purified than the corresponding compound with a non-methylated amine.<sup>28</sup>

## Experimental Section

**Synthesis.** The complexes [Ru(TAP)<sub>2</sub>POQ–Nmet]<sup>2+</sup>, [Ru(BPY)<sub>2</sub>POQ–Nmet]<sup>2+</sup>, [Ru(TAP)<sub>2</sub>acPhen]<sup>2+</sup>, and [Ru(BPY)<sub>2</sub>acPhen]<sup>2+</sup> have been prepared by refluxing the precursors Ru(TAP)<sub>2</sub>Cl<sub>2</sub> or Ru(BPY)<sub>2</sub>Cl<sub>2</sub><sup>31</sup> and the ligands POQ–Nmet or acPhen in MeOH/H<sub>2</sub>O 1:1 under argon, according to the methods described previously.<sup>28</sup> The syntheses of [Ru(TAP)<sub>2</sub>Phen]<sup>2+</sup> and [Ru(BPY)<sub>2</sub>Phen]<sup>2+</sup><sup>32</sup> have already been described.

The preparation of POQ–Nmet (5-[4-[N-methyl-N-(7-chloroquinolin-4-yl)amino]-2-thiabutanecarboxamido]-1,10-phenanthroline), acPhen (5-acetamido-1,10-phenanthroline) and Nmet–

\* Corresponding author; Tel, + 32 2 650 3017; Fax, + 32 2 650 3606; E-mail, akirsch@ulb.ac.be.

<sup>†</sup> Director of Research at the FNRS, Belgium.

<sup>®</sup> Abstract published in *Advance ACS Abstracts*, August 1, 1997.

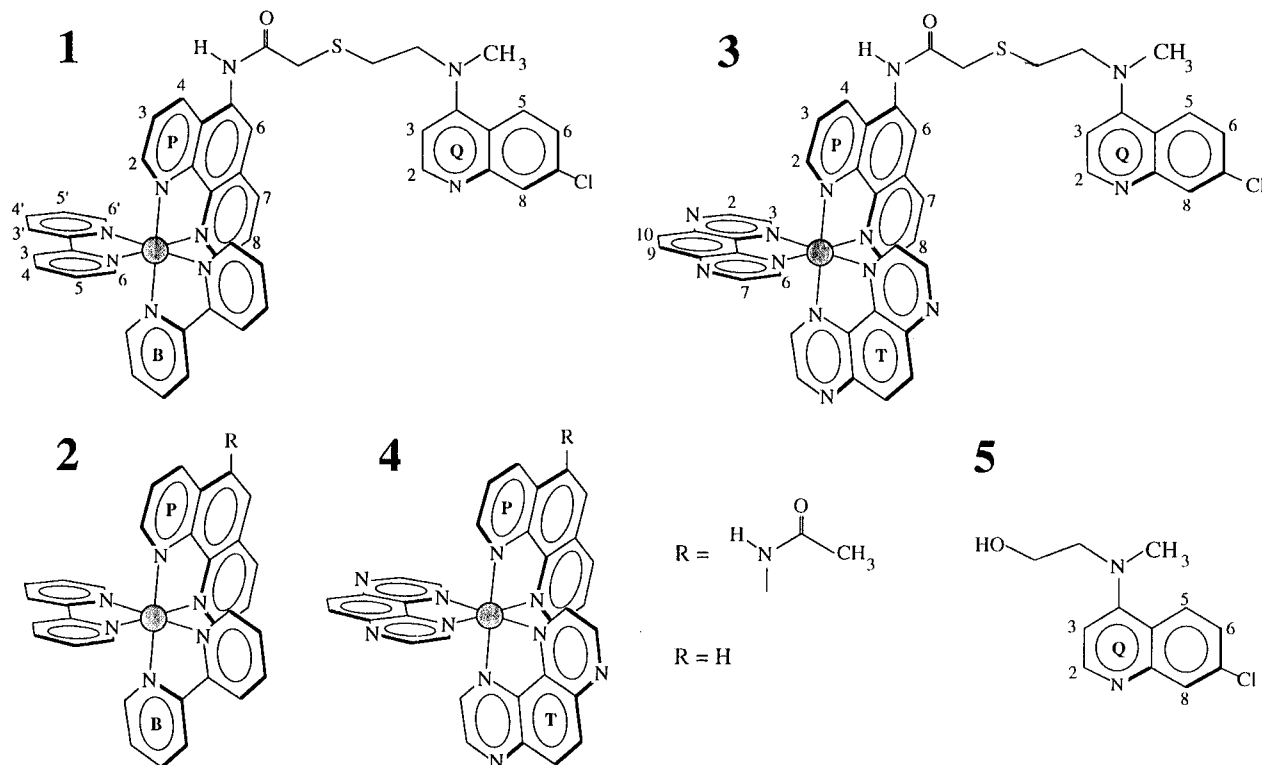


**Figure 1.** (1)  $[\text{Ru}(\text{BPY})_2\text{POQ-Nmet}]^{2+}$  (BPY = 2,2'-bipyridine, POQ-Nmet = 5-[4-[N-methyl-N-(7-chloroquinolin-4-yl)amino]-2-thiabutanecarboxamido]-1,10-phenanthroline), (2)  $[\text{Ru}(\text{BPY})_2\text{Phen-R}]^{2+}$  (R = acetamido, acPhen = 5-acetamido-1,10-phenanthroline or R = H, Phen = 1,10-phenanthroline), (3)  $[\text{Ru}(\text{TAP})_2\text{POQ-Nmet}]^{2+}$  (TAP = 1,4,5,8-tetraazaphenanthrene), (4)  $[\text{Ru}(\text{TAP})_2\text{Phen-R}]^{2+}$  (R = acetamido or H) and (5) Nmet-quinoline (4-[N-methyl-N-(2-hydroxyethyl)amino]-7-chloroquinoline).

quinoline (4-[N-methyl-N-(2-hydroxyethyl)amino]-7-chloroquinoline) will be described elsewhere.<sup>33</sup>

**Purity and Characterization.** The purity of the different complexes has been tested by HPLC (Waters 991 instrument, Bondapak C18 column, gradient of MeOH/H<sub>2</sub>O, pH 2.5 with phosphoric acid).<sup>34</sup>

The complexes and the Nmet-quinoline have been characterized by <sup>1</sup>H NMR and electrospray mass spectrometry (ESMS). The NMR have been recorded in DMSO-*d*<sub>6</sub> at 300 K with a 250, 360, or 600 MHz spectrometer. The assignments of the different peaks have been made from the corresponding <sup>1</sup>H-<sup>1</sup>H COSY 360 MHz correlation spectra and from comparisons with reference complexes (for the numbering of the protons, see Figure 1):  $[\text{Ru}(\text{TAP})_2\text{POQ-Nmet}]^{2+}$ , 600 MHz, <sup>1</sup>H-<sup>1</sup>H COSY (360 MHz),  $\delta$  9.04/9.07 (ppm) (4 H, d, T<sub>2,2',7,7'</sub>),  $\delta$  8.65 (4 H, s, T<sub>9,9',10,10'</sub>),  $\delta$  8.32/8.26/8.53/8.51 (4 H, d, T<sub>3,3',6,6'</sub>),  $\delta$  9.48/8.76 (2 H, d, P<sub>4,7</sub>),  $\delta$  8.18/8.31 (2 H, d, P<sub>2,9</sub>),  $\delta$  7.79/7.73 (2 H, dd, P<sub>3,8</sub>),  $\delta$  8.62 (1 H, d, P<sub>6</sub>),  $\delta$  8.11 (1 H, d, Q<sub>8</sub>),  $\delta$  8.35 (1 H, d, Q<sub>5</sub>),  $\delta$  7.54 (1 H, dd, Q<sub>6</sub>),  $\delta$  8.47 (1 H, d, Q<sub>2</sub>),  $\delta$  7.15 (1 H, d, Q<sub>3</sub>),  $\delta$  11.65 (1 H, s, NH).  $[\text{Ru}(\text{BPY})_2\text{POQ-Nmet}]^{2+}$ , 360 MHz, <sup>1</sup>H-<sup>1</sup>H COSY,  $\delta$  8.82/8.86 (ppm) (4 H, d, B<sub>3,3',3'',3'''</sub>),  $\delta$  8.10/8.21 (4 H, dd, B<sub>4,4',4'',4'''</sub>),  $\delta$  7.32/7.59 (4 H, dd, B<sub>5,5',5'',5'''</sub>),  $\delta$  7.59/7.83 (4 H, d, B<sub>6,6',6'',6'''</sub>),  $\delta$  9.06/8.71 (4 H, d, P<sub>4,7</sub>),  $\delta$  8.16/8.04 (2 H, d, P<sub>2,9</sub>),  $\delta$  7.89/7.83 (2 H, dd, P<sub>3,8</sub>),  $\delta$  8.59 (1 H, d, P<sub>6</sub>),  $\delta$  7.89 (1 H, d, Q<sub>8</sub>),  $\delta$  8.25 (1 H, d, Q<sub>5</sub>),  $\delta$  7.49 (1 H, dd, Q<sub>6</sub>),  $\delta$  8.52 (1 H, d, Q<sub>2</sub>),  $\delta$  7.07 (1 H, d, Q<sub>3</sub>),  $\delta$  10.90 (1 H, s, NH).  $[\text{Ru}(\text{TAP})_2\text{acPhen}]^{2+}$ , 360 MHz,  $\delta$  9.05 (ppm) (4 H, d, T<sub>2,2',7,7'</sub>),  $\delta$  8.65 (4 H, s, T<sub>9,9',10,10'</sub>),  $\delta$  8.24/8.23/8.49/8.47 (4 H, d, T<sub>3,3',6,6'</sub>),  $\delta$  8.97/8.79 (2 H, d, P<sub>4,7</sub>),  $\delta$  8.16/8.29 (2 H, d, P<sub>2,9</sub>),  $\delta$  7.82/7.73 (2 H, dd, P<sub>3,8</sub>),  $\delta$  8.66 (1 H, d, P<sub>6</sub>),  $\delta$  10.48 (1 H, s, NH).  $[\text{Ru}(\text{BPY})_2\text{acPhen}]^{2+}$ , 360 MHz,  $\delta$  8.82/8.86 (ppm) (4 H, d, B<sub>3,3',3'',3'''</sub>),  $\delta$  8.10/8.21 (4 H, dd, B<sub>4,4',4'',4'''</sub>),  $\delta$  7.36/7.57 (4 H, dd, B<sub>5,5',5'',5'''</sub>),  $\delta$  7.56/7.82 (4 H, d, B<sub>6,6',6'',6'''</sub>),  $\delta$  8.94/8.73 (4 H, d, P<sub>4,7</sub>),  $\delta$  8.15/8.02 (2 H, d, P<sub>2,9</sub>),  $\delta$  7.90/7.82 (2 H, dd, P<sub>3,8</sub>),  $\delta$  8.64 (1 H, d, P<sub>6</sub>),  $\delta$  10.43 (1 H, s, NH). Nmet-

quinoline, 360 MHz,  $\delta$  7.91 (1 H, d, Q<sub>8</sub>),  $\delta$  8.29 (1 H, d, Q<sub>5</sub>),  $\delta$  7.47 (1 H, dd, Q<sub>6</sub>),  $\delta$  8.59 (1 H, d, Q<sub>2</sub>),  $\delta$  6.93 (1 H, d, Q<sub>3</sub>).

The electrospray mass spectra have been obtained with extraction cone voltages of 65 and 80 V; they have been recorded in the laboratory of Pr. A. van Dorsselaer, at the University L. Pasteur, Strasbourg, France. The spectra of the different complexes have been recorded in H<sub>2</sub>O/MeCN 50:50.  $[\text{Ru}(\text{TAP})_2\text{POQ-Nmet}]^{2+}$  (Cl<sup>-</sup>)<sub>2</sub> (*M*<sub>w</sub> = 1022.81) exhibits essentially peaks at *m/z* = 476.64 (intensity *I* = 35, M-2Cl<sup>-</sup> calculated: 476.43) and at *m/z* = 318.24 (*I* = 100, [M + H<sup>+</sup>] - 2Cl<sup>-</sup> calculated: 317.96).  $[\text{Ru}(\text{BPY})_2\text{POQ-Nmet}]^{2+}$  (*M*<sub>w</sub> = 970.82) displays peaks at *m/z* = 450.81 (*I* = 100, M-2Cl<sup>-</sup>, calculated: 450.44) and at *m/z* = 301.00 (*I* = 95, [M + H<sup>+</sup>] - 2Cl<sup>-</sup> calculated: 300.63). For  $[\text{Ru}(\text{TAP})_2\text{acPhen}]^{2+}$  (*M*<sub>w</sub> = 772.63) a peak is detected at *m/z* = 351.55 (M-2Cl<sup>-</sup> calculated: 351.35). The assignments of the peaks and of the corresponding charges have been tested by high-resolution measurements carried out on these peaks and by analyzing the isotopic distribution (the correspondence between the calculated and measured distribution is given in Supporting Information for *m/z* = 476.6, for an example). The ESMS data reveal clearly for the two bifunctional complexes the presence of protonated species. For  $[\text{Ru}(\text{TAP})_2\text{POQ-Nmet}]^{2+}$  (Cl<sup>-</sup>)<sub>2</sub>, a peak at 476.64, which corresponds to *m/z* for  $[\text{Ru}(\text{TAP})_2\text{POQ-Nmet}]^{2+}$ , is observed as well as another peak at 318.24, which corresponds to *m/z* of the same complex and thus to the protonated species  $[\text{Ru}(\text{TAP})_2\text{POQ-Nmet}+\text{H}]^{3+}$ .

**Chemicals.** The phosphate buffers were adjusted to the correct pH (at room temperature) by mixing equimolar solutions of Na<sub>2</sub>HPO<sub>4</sub> and NaH<sub>2</sub>PO<sub>4</sub> (Aldrich, A.C.S. reagent, in MilliQ water). The tris buffers were prepared by adding concentrated HCl to aqueous solutions of tris(hydroxymethyl)aminomethane (Sigma, 99.9%). Methanol and acetone were freshly distilled, and acetonitrile, DMSO (Aldrich HPLC grade), and DMF (Fluka, 99%) were used as received. When specified, the

**TABLE 1: Electronic Absorption Data:  $\lambda_{\text{max}}$  of Absorption (in nm,  $\pm 1$  nm) and Most Significant Shoulders (S) for the Different Complexes, Nmet–Quinoline and Phenanthroline-Based Ligands in Aqueous Solution and/or in Acetonitrile<sup>a</sup>**

complex	solvent	UV				visible	
		$\lambda$	$\lambda$	$\lambda$	$\lambda$	$\lambda$	$\lambda$
[Ru(TAP) <sub>2</sub> POQ–Nmet] <sup>2+</sup>	H <sub>2</sub> O <sup>b</sup>	202 (8.27)	218 (S) (7.45)	272 (6.59)	354 (1.78)	414 (1.53)	460 (1.32)
[Ru(TAP) <sub>2</sub> acPhen] <sup>2+</sup>		202 (8.18)		272 (6.83)		414 (1.69)	460 (1.43)
[Ru(TAP) <sub>2</sub> Phen] <sup>2+</sup>		202 (9.58)		272 (7.16)		412 (1.65)	466 (1.43)
[Ru(BPY) <sub>2</sub> POQ–Nmet] <sup>2+</sup>		222 (6.61)	272 (6.07)	284 (6.02)	354 (1.73)	426 (S) (1.34)	452 (1.50)
[Ru(BPY) <sub>2</sub> acPhen] <sup>2+</sup>			272 (5.34)	284 (5.86)		426 (S) (1.35)	450 (1.51)
[Ru(BPY) <sub>2</sub> Phen] <sup>2+</sup>			264 (5.44)	286 (6.24)		426 (S) (1.40)	450 (1.59)
Nmet–quinoline			224 (3.31)		354 (1.11)		
[Ru(TAP) <sub>2</sub> POQ–Nmet] <sup>2+</sup>	MeCN <sup>c</sup>		224	272	354	416	458
[Ru(TAP) <sub>2</sub> acPhen] <sup>2+</sup>		200		272		416	458
[Ru(TAP) <sub>2</sub> Phen] <sup>2+</sup>		200		272		414	458
[Ru(BPY) <sub>2</sub> POQ–Nmet] <sup>2+</sup>	MeCN	222	278	284	354	427 (S)	450
[Ru(BPY) <sub>2</sub> acPhen] <sup>2+</sup>			278	284		427 (S)	450
[Ru(BPY) <sub>2</sub> Phen] <sup>2+</sup>			264	286		427 (S)	448
Nmet–quinoline	MeCN <sup>c</sup>		222		354		
Nmet–quinoline	MeCN <sup>d</sup>		222	250 (S)	328		
Phen	H <sub>2</sub> O			264			
acPhen				267			

<sup>a</sup> The molar extinction coefficients (in 10<sup>4</sup> M<sup>-1</sup> cm<sup>-1</sup>,  $\pm 10\%$ ) are in parentheses. <sup>b</sup> pH 4.5 (10<sup>-3</sup> M H<sub>2</sub>PO<sub>4</sub><sup>-</sup>). <sup>c</sup> In the presence of methanesulfonic acid (2  $\times$  10<sup>-5</sup> M). <sup>d</sup> In the presence of piperidine (4  $\times$  10<sup>-5</sup> M).

solutions were purged by argon for at least 20–30 min before measurements were taken.

**Absorption and Emission Spectroscopy.** Absorption spectra were recorded on a HP 8452A UV–vis diode array spectrometer. The molar extinction coefficients of the complexes in aqueous solution were determined by ruthenium titration by atomic emission from plasma atomisation (spectrometric Spectrospan IV instrument).<sup>35</sup>

The emission spectra were obtained with a Shimadzu RF-5001 PC spectrofluorimeter equipped with a Hamamatsu R-928 red sensitive photomultiplier tube and were corrected for the instrument response. The relative emission quantum yields were determined by integrating the emission spectra over the frequency.

The emission lifetimes were determined with a modified Applied Photophysics laser kinetic spectrometer equipped with a Hamamatsu R-928 photomultiplier tube. The excitation source is composed of a frequency-doubled Nd:YAG laser (Continuum NY 61-10) coupled with a dye laser (Continuum ND60, dye DCM,  $\lambda_{\text{exc}}$  = 640 nm) and with the mixing option (Continuum UVX), producing a 400 nm beam (10 ns pulse width, maximum of 27 mJ/pulse, used at ca. 8 mJ/pulse). Kinetic analyzes of the luminescence decays were performed by nonlinear least-squares regressions using a modified Marquardt's algorithm.<sup>36,37</sup>

Some emission lifetimes were measured by time-resolved single-photon counting (SPC) with a FL-900 Edinburgh Instruments spectrometer (Edinburgh, U.K.) equipped with a nitrogen-filled discharge lamp (with gas pressure between 0.25 and 0.4 bar, a 1.5 mm gap, and 5.6 kV between electrodes) and a Peltier-cooled Hamamatsu R-955 photomultiplier tube. The emission decays were analyzed with the Edinburgh Instruments software (version 3.00), based on nonlinear least-squares regressions using a modified Marquardt's algorithm. The temperature of the solutions was thermostated at 22 °C.

Laser flash photolysis experiments were carried out using the pulsed Nd:YAG laser mentioned above, with maximum power at 400 nm (ca. 27 mJ), and the Applied Photophysics laser kinetic spectrometer described previously.<sup>20</sup> Limitations on the lower accessible timescale are due to the response time of the detection system (minimum RC time constant  $\approx$  12 ns).

Global analyses were carried out on the emission decays of [Ru(TAP)<sub>2</sub>POQ–Nmet]<sup>2+</sup> in the laboratory of Pr. De Schryver (KULeuven) on a SPC equipment with picosecond laser

excitation (425 nm) and a multichannel plate for the detection. The decays were analyzed with a global analyses program written by N. Boens<sup>38</sup> so as to show that the two detected species correspond to the same luminophore.

## Results

**UV–Vis Absorption Spectroscopy.** The spectroscopic properties have also been examined in aqueous solution at different pH's in order to evidence changes with pH. The ESMS spectra exhibit indeed the presence of protonated species. Moreover a careful examination of the <sup>1</sup>H NMR data<sup>33</sup> has shown that, when the quinoline unit is nonprotonated, the bifunctional complex can exist in a folded conformation. In contrast, when the quinoline unit is protonated, the complex is unfolded.

Therefore, the UV–vis absorption spectra have been recorded not only in different organic solvents but also in aqueous solution for the mono- and bifunctional Ru(II) complexes and for the Nmet–quinoline (Table 1).

**Monofunctional Complexes** ([Ru(BPY)<sub>2</sub>Phen]<sup>2+</sup>, [Ru(BPY)<sub>2</sub>acPhen]<sup>2+</sup>, [Ru(TAP)<sub>2</sub>Phen]<sup>2+</sup>, [Ru(TAP)<sub>2</sub>acPhen]<sup>2+</sup>), and the Nmet–Quinoline (Figure 1). The amido function on the ligand in the complexes influences their absorption mainly in the UV region (between 220–290 and 300–400 nm) (Figure 2). Moreover, in aqueous solution, the spectra of these complexes do not change with pH (in the range 3–10), in contrast to the absorptions of Nmet–quinoline (Figure 3) which, after treatment of the data, led to a pK<sub>a</sub> of 7.1. In acetonitrile the absorption also changes upon addition of an acid (methanesulfonic acid) or a base (piperidine). The acid produces a strong hyperchromic effect on the band at 354 nm due to protonation of the aromatic nitrogen.<sup>39</sup>

**Bifunctional Complexes.** The comparison of the absorptions of the bifunctional complexes [Ru(BPY)<sub>2</sub>POQ–Nmet]<sup>2+</sup> and [Ru(TAP)<sub>2</sub>POQ–Nmet]<sup>2+</sup> (Figure 1) with those of each separated unit shows that the spectroscopic characteristics of the two units in aqueous solution at pH 4.5 are additive (within experimental error) (Figure 2). Moreover, the spectra of the bifunctional complexes also exhibit a strong pH dependence due to the quinoline unit. From the change in absorption of [Ru(TAP)<sub>2</sub>POQ–Nmet]<sup>2+</sup> at 354 nm with pH (Figure 4), a pK<sub>a</sub> for the quinoline unit chemically attached to the metallic unit can be determined (pK<sub>a</sub> = 6.1); this value is lower than that for

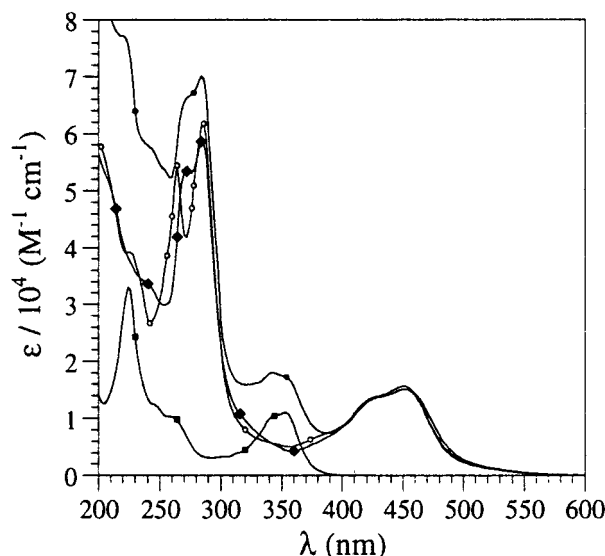


**Figure 2.** Absorption spectra for (solid circle)  $[\text{Ru}(\text{BPY})_2\text{POQ-Nmet}]^{2+}$ , (solid diamond)  $[\text{Ru}(\text{BPY})_2\text{acPhen}]^{2+}$ , (open circle)  $[\text{Ru}(\text{BPY})_2\text{Phen}]^{2+}$  and (crossed square) Nmet-quinoline in aqueous solution, 1 mM  $\text{NaH}_2\text{PO}_4$  (pH 4.5).

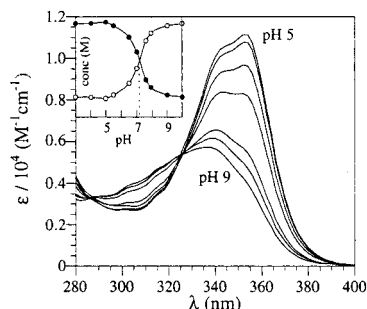


**Figure 3.** Changes of the absorption spectrum of the Nmet-quinoline (Figure 1) with increasing pH (aqueous solution, 1 mM phosphate buffer): pH, 5, 5.5, 6.5, 7, 7.5, 8, and 9. Inset: Variation of the concentration of protonated (solid circle) ( $\epsilon = 1.13 \times 10^4 \text{ M}^{-1} \text{ cm}^{-1}$ ) and nonprotonated (open circle) ( $\epsilon = 3.9 \times 10^3 \text{ M}^{-1} \text{ cm}^{-1}$ ) Nmet-quinoline, calculated from the  $\epsilon$  at 354 nm; the intersection gives a  $\text{pK}_a$  of 7.1.

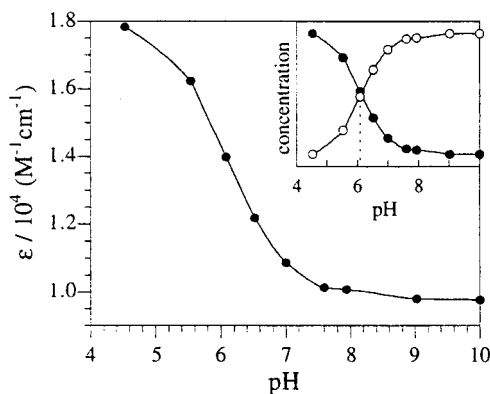


**Figure 4.** Variation of the molar absorption coefficient at 354 nm of  $[\text{Ru}(\text{TAP})_2\text{POQ-Nmet}]^{2+}$  with the pH (aqueous solution, 1 mM phosphate buffer). Inset: Concentrations of protonated (solid circle) ( $\epsilon = 1.79 \times 10^4 \text{ M}^{-1} \text{ cm}^{-1}$ ) and nonprotonated (open circle) ( $9.9 \times 10^3 \text{ M}^{-1} \text{ cm}^{-1}$ ) form, calculated from the  $\epsilon$  at 354 nm; the intersection gives a  $\text{pK}_a$  of 6.1.

the free Nmet-quinoline. This indicates that the acid-base properties of the Nmet-quinoline are altered by the presence of the metal complex unit. In contrast, the absorption characteristics of the metallic unit are not influenced by the attachment of the aminoquinoline part.

**Luminescence Spectroscopy.** The emission data ( $\lambda_{\text{max}}$  of emission, relative emission quantum yields  $\Phi_{\text{em}}^{\text{rel}}$ , and luminescence lifetimes) from the  $^3\text{MLCT}$  state of the bifunctional complexes  $[\text{Ru}(\text{L})_2\text{POQ-Nmet}]^{2+}$  ( $\text{L} = \text{BPY}$  or  $\text{TAP}$ ) in different solvents are presented in Tables 2–4. They are compared with those of the corresponding monofunctional compounds  $[\text{Ru}(\text{L})_2\text{Phen}]^{2+}$  or  $[\text{Ru}(\text{L})_2\text{acPhen}]^{2+}$ . The  $\Phi_{\text{em}}^{\text{rel}}$  are measured relative to the emission of the monofunctional complexes. The emission intensity of  $[\text{Ru}(\text{BPY})_2\text{Phen}]^{2+}$  is slightly lower and the luminescence lifetime slightly shorter than that for  $[\text{Ru}(\text{BPY})_2\text{acPhen}]^{2+}$  (Table 2). In contrast, the emission and luminescence lifetime of  $[\text{Ru}(\text{TAP})_2\text{Phen}]^{2+}$  are not affected by the attached acetamido group (Table 3).

**Bifunctional Complexes in Organic Solutions.** *Emission Spectra and Quantum Yields.* The bifunctional complex  $[\text{Ru}(\text{BPY})_2\text{POQ-Nmet}]^{2+}$  (Table 2) exhibits the same emission maxima and luminescence quantum yields as those of the corresponding monofunctional species  $[\text{Ru}(\text{BPY})_2\text{acPhen}]^{2+}$ . Thus the presence of the quinoline unit does not alter the emission properties of the complex moiety.

For  $[\text{Ru}(\text{TAP})_2\text{POQ-Nmet}]^{2+}$ , although its emission maxima are the same as those of  $[\text{Ru}(\text{TAP})_2\text{Phen}]^{2+}$  and  $[\text{Ru}(\text{TAP})_2\text{acPhen}]^{2+}$  (Table 3), its emission quantum yield is much lower, while the addition of an acid or a base to the solvent (MeCN) strongly influences  $\Phi_{\text{em}}^{\text{rel}}$ . An 85% luminescence drop is observed by addition of pyridine, and 100% of emission is restored by addition of an excess of methanesulfonic acid.

*Luminescence Lifetimes.* When excited by a laser pulse, the luminescence of  $[\text{Ru}(\text{BPY})_2\text{POQ-Nmet}]^{2+}$  decays according to single exponentials in all the solvents and the corresponding lifetimes are equal to those of excited  $[\text{Ru}(\text{BPY})_2\text{acPhen}]^{2+}$  (Table 2). In contrast, excited  $[\text{Ru}(\text{TAP})_2\text{POQ-Nmet}]^{2+}$  decays biexponentially in all of the organic solvents examined.

$$I(t) = A_{\text{short}} e^{-t/\tau_{\text{short}}} + A_{\text{long}} e^{-t/\tau_{\text{long}}}$$

Global analyses of the SPC data in  $\text{CH}_3\text{CN}$  show that the short and long decay components are associated with the same type of luminophore (same emission spectra), which is characteristic of the metallic unit. Moreover, the long decay component always exhibits an associated rate constant which corresponds to the excited  $[\text{Ru}(\text{TAP})_2\text{acPhen}]^{2+}$  and  $[\text{Ru}(\text{TAP})_2\text{Phen}]^{2+}$  (Tables 3 and 4). A linear correlation is clearly obtained when the long decay component of excited  $[\text{Ru}(\text{TAP})_2\text{POQ-Nmet}]^{2+}$  is plotted versus the lifetime of excited  $[\text{Ru}(\text{TAP})_2\text{Phen}]^{2+}$  for different solvents. In contrast, the short decay component of  $[\text{Ru}(\text{TAP})_2\text{POQ-Nmet}]^{2+}$  may be shorter than that for  $[\text{Ru}(\text{TAP})_2\text{Phen}]^{2+}$  by a factor of 2 to 25 depending on the solvent. Moreover, the relative contributions of the two components depend on the solvent and on the presence of an acid or a base. As shown by absorption and NMR spectroscopy,<sup>33</sup> the addition of an acid or a base determines the degree of protonation of the aminoquinoline unit. Therefore, when excited  $[\text{Ru}(\text{TAP})_2\text{POQ-Nmet}]^{2+}$  in acetonitrile is titrated with methanesulfonic acid (concentration range from 0 to  $1.6 \times 10^{-5} \text{ M}$ , for a complex concentration of  $1.2 \times 10^{-5} \text{ M}$ ) the contribution of the long-lived species increases (Figure 5). The decay becomes monoexponential upon addition of excess acid, with a lifetime identical to that for excited  $[\text{Ru}(\text{TAP})_2\text{acPhen}]^{2+}$  (Figure 5). With an excess of piperidine (causing deprotonation of the aminoquinoline unit), the emission decay becomes a quasi single exponential<sup>34</sup> with a much shorter lifetime than excited  $[\text{Ru}(\text{TAP})_2\text{acPhen}]^{2+}$ .

**Bifunctional Complexes in Aqueous Solutions.** *Emission Intensities.* The luminescence of  $[\text{Ru}(\text{BPY})_2\text{POQ-Nmet}]^{2+}$  is pH independent (in the pH range 4–9, i.e., as observed for  $[\text{Ru}$

**TABLE 2: Emission Data for the BPY Complexes in Different Solvents<sup>a</sup>**

solvent	[Ru(BPY) <sub>2</sub> POQ–Nmet] <sup>2+</sup>				[Ru(BPY) <sub>2</sub> acPhen] <sup>2+</sup>				[Ru(BPY) <sub>2</sub> Phen] <sup>2+ b</sup>			
	$\lambda_{\max}$ (nm)	$\Phi_{\text{em}}^{\text{rel}}$	$\tau_{\text{air}}$ (ns)	$\tau_{\text{Ar}}$ (ns)	$\lambda_{\max}$ (nm)	$\Phi_{\text{em}}^{\text{rel}}$	$\tau_{\text{air}}$ (ns)	$\tau_{\text{Ar}}$ (ns)	$\lambda_{\max}$ (nm)	$\Phi_{\text{em}}^{\text{rel}}$	$\tau_{\text{air}}$ (ns)	$\tau_{\text{Ar}}$ (ns)
H <sub>2</sub> O <sup>c</sup>	616	115	600	1120	615	107	480	890	616	100	420	720
CH <sub>3</sub> OH	613	106	195	765	613	103	190		614	100	180	625
(CH <sub>3</sub> ) <sub>2</sub> CO	617	105	185	1000	616	106	190	950	617	100	170	840
CH <sub>3</sub> CN	614	105	150	965	613	105	145	970	614	100	140	820
DMSO	627	94 <sup>d</sup>	450	1100	625	93 <sup>d</sup>	445	1050	624	100	410	955
DMF	622	92 <sup>d</sup>	240	1100	621	103 <sup>d</sup>	245	1065	622	100	235	970

<sup>a</sup> Emission maxima ( $\pm 1$  nm) (corrected spectra), relative emission quantum yields (in %,  $\pm 3\%$ ; [Ru(BPY)<sub>2</sub>Phen]<sup>2+</sup> is taken as 100% in all the solvents under air) and luminescence lifetimes ( $\pm 2\%$ ). <sup>b</sup> For data concerning [Ru(BPY)<sub>2</sub>Phen]<sup>2+</sup>, see also ref 3. <sup>c</sup> The same results have been obtained in H<sub>2</sub>O, at pH 4.5 (1 mM H<sub>2</sub>PO<sub>4</sub><sup>−</sup>), and at pH 9.1 (1 mM HPO<sub>4</sub><sup>2−</sup>). <sup>d</sup> There are problems of reproducibility in DMSO and DMF, and therefore, a higher error should be associated to these values.

**TABLE 3: Emission Data for the TAP Complexes in Different Solvents<sup>a</sup>**

solvent	[Ru(TAP) <sub>2</sub> POQ–Nmet] <sup>2+</sup>				[Ru(TAP) <sub>2</sub> Phen] <sup>2+</sup>			
	$\lambda_{\max}$ (nm)	$\Phi_{\text{em}}^{\text{rel}}$	$\lambda_{\max}$ (nm)	$\Phi_{\text{em}}^{\text{rel}}$	$\tau_{\text{air}}$ (ns)	$\tau_{\text{Ar}}$ (ns)		
H <sub>2</sub> O (pH 4.5)	645	100	645	100 <sup>b</sup>	630 <sup>b</sup>			
H <sub>2</sub> O (pH 9.1)	645	4	645	100 <sup>b</sup>	740 <sup>b</sup>	910 <sup>c</sup>		
CH <sub>3</sub> OH	620		620		560	1590		
(CH <sub>3</sub> ) <sub>2</sub> CO	634	24 <sup>d</sup>	635	100	740	2440		
CH <sub>3</sub> CN	629	15–100 <sup>e</sup>	629	100	700 <sup>b</sup>	2560		
DMSO	645	50 <sup>d</sup>	645	100	960	2020		
DMF	648	79 <sup>d</sup>	648	100	650	1600		

<sup>a</sup> Emission maxima ( $\pm 1$  nm) (corrected spectra), relative emission quantum yields ( $\Phi_{\text{em}}^{\text{rel}}$ , in %,  $\pm 3\%$ ; [Ru(TAP)<sub>2</sub>Phen]<sup>2+</sup> is taken as 100% in all the solvents) and luminescence lifetimes ( $\pm 2\%$ ). <sup>b</sup> The same  $\Phi_{\text{em}}^{\text{rel}}$  and lifetimes have been obtained for [Ru(TAP)<sub>2</sub>acPhen]<sup>2+</sup>. <sup>c</sup> Obtained in water (pH  $\approx$  5–6), and  $\tau_{\text{air}} = 730$  ns. <sup>d</sup> Obtained in the absence of added acid or base. <sup>e</sup> 15%, with an excess of pyridine; 100%, with an excess of methanesulfonic acid.

(BPY)<sub>2</sub>Phen]<sup>2+</sup> and [Ru(BPY)<sub>2</sub>acPhen]<sup>2+</sup>). In contrast, the emission of the TAP complexes (bi- and even monofunctional) decreases with increasing acidity. This is due to protonation of the excited complex on the TAP ligands<sup>40</sup> so that the luminescence of [Ru(TAP)<sub>2</sub>acPhen]<sup>2+</sup> (Figure 6a) starts decreasing from pH 5 to 6.<sup>41</sup> For excited [Ru(TAP)<sub>2</sub>POQ–Nmet]<sup>2+</sup>, two sites of protonation thus exist, on the TAP ligands as explained above and on the quinoline unit. Therefore, in order to examine the effect of protonation on the luminescence (caused only by protonation of the organic part) the ratios of  $\Phi_{\text{em}}$

**TABLE 4: Luminescence Lifetimes of [Ru(TAP)<sub>2</sub>POQ–Nmet]<sup>2+</sup> ( $\pm 5\%$ ) in Various Solvents. Preexponential Factors in Parentheses**

		[Ru(TAP) <sub>2</sub> POQ–Nmet] <sup>2+</sup>			
solvent		$\tau_{\text{short}}$ (ns)	(%)	$\tau_{\text{long}}$ (ns)	(%)
CH <sub>3</sub> OH	air	50	(35)	540	(65)
	Ar	60	(45)	1410	(55)
(CH <sub>3</sub> ) <sub>2</sub> CO	air	150	(50)	710	(50)
	Ar	200	(50)	1990 <sup>a</sup>	(50)
CH <sub>3</sub> CN	air	110	(50)	650	(50)
	Ar	115	(65)	1840 <sup>a</sup>	(35)
DMSO	air	290	(60)	950	(40)
	Ar	335	(70)	1800	(30)
DMF	air	265	(55)	650	(45)
	Ar	355	(70)	1600	(30)

<sup>a</sup> For these long decay components, obtained from a biexponential fitting under laser excitation, where the ratio  $\tau_{\text{long}}/\tau_{\text{short}} \gg 10$ , a systematic underestimation of the lifetimes is obtained (error 20%).

between [Ru(TAP)<sub>2</sub>POQ–Nmet]<sup>2+</sup> and [Ru(TAP)<sub>2</sub>acPhen]<sup>2+</sup> (measured in exactly the same conditions) have been plotted versus pH (Figure 6b). This ratio is equal to 1 in acid solution (Figure 6b) but decreases in basic solution with an inflection point at pH 5.8 (Figure 6b), a value comparable to the  $pK_a$  of the aminoquinoline unit ( $pK_a = 6.1$ ). This behavior suggests that the emission from the metallic unit is quenched when the organic unit is deprotonated.

**Luminescence Lifetimes.** For the TAP monofunctional complex, the pH dependence of the luminescence lifetimes is

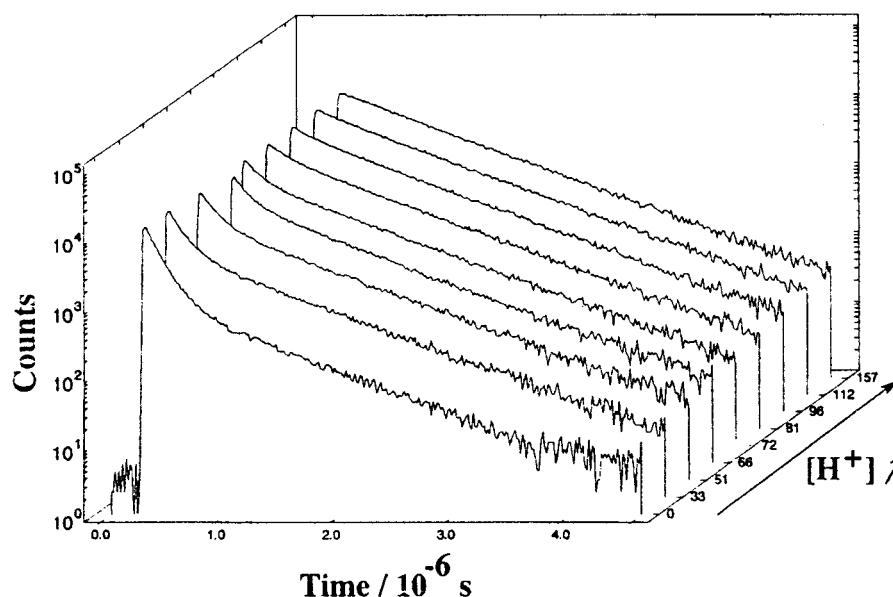


**Figure 5.** Luminescence decays of [Ru(TAP)<sub>2</sub>POQ–Nmet]<sup>2+</sup> after pulsed excitation with increasing concentrations of methanesulfonic acid (in 10<sup>−7</sup> M) in acetonitrile.

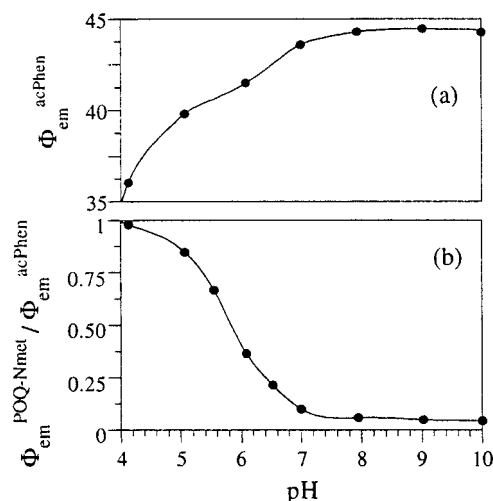


**Figure 6.** (a) Emission quantum yields (in au) of  $[\text{Ru}(\text{TAP})_2\text{acPhen}]^{2+}$  versus the pH, phosphate buffer 1 mM. (b) Relative emission quantum yields versus the pH of  $[\text{Ru}(\text{TAP})_2\text{POQ-Nmet}]^{2+}$  relative to that of  $[\text{Ru}(\text{TAP})_2\text{acPhen}]^{2+}$ .

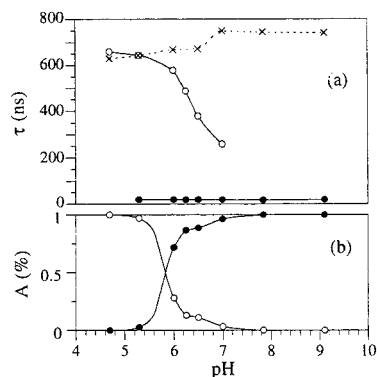


**Figure 7.** (a) Luminescence lifetimes versus the pH, for  $[\text{Ru}(\text{TAP})_2\text{POQ-Nmet}]^{2+}$  and  $[\text{Ru}(\text{TAP})_2\text{acPhen}]^{2+}$ : (dark circle) short  $\tau$  for  $[\text{Ru}(\text{TAP})_2\text{POQ-Nmet}]^{2+}$ , (open circle) long  $\tau$  for  $[\text{Ru}(\text{TAP})_2\text{POQ-Nmet}]^{2+}$ , ( $\times$ )  $\tau$  for  $[\text{Ru}(\text{TAP})_2\text{acPhen}]^{2+}$ . (b) Preexponential factors for the luminescence decays of  $[\text{Ru}(\text{TAP})_2\text{POQ-Nmet}]^{2+}$  versus the pH: (solid circle) factor for short  $\tau$ , (open circle) factor for long  $\tau$ .

attributed, as above for the emission quantum yields,<sup>42</sup> to protonation on the TAP ligands.

For the bifunctional  $[\text{Ru}(\text{BPY})_2\text{POQ-Nmet}]^{2+}$  no pH dependence is observed. For  $[\text{Ru}(\text{TAP})_2\text{POQ-Nmet}]^{2+}$  the luminescence decays biexponentially after pulsed excitation, in phosphate and in tris buffer. In Figure 7 the corresponding lifetimes ( $\tau_{\text{short}}$  and  $\tau_{\text{long}}$ ) (Figure 7a) and the normalized preexponential factors (Figure 7b) are plotted as a function of the pH. When the pH increases above 4.5 the contribution ( $A\%$ ) corresponding to  $\tau_{\text{long}}$  decreases and a corresponding increase for  $\tau_{\text{short}}$  is observed (Figure 7b). An inflection point is observed at pH 5.8, i.e., in the same pH domain as that of the inflection point for the emission intensities and for the absorption of  $[\text{Ru}(\text{TAP})_2\text{POQ-Nmet}]^{2+}$  versus the pH. In acidic and basic solutions the decays become single exponentials. The lifetimes correspond to 660 ns at pH 4.5 as those for excited  $[\text{Ru}(\text{TAP})_2\text{acPhen}]^{2+}$ , and to 17 ns at pH 9 as compared to those for 740 ns observed for excited  $[\text{Ru}(\text{TAP})_2\text{acPhen}]^{2+}$ .

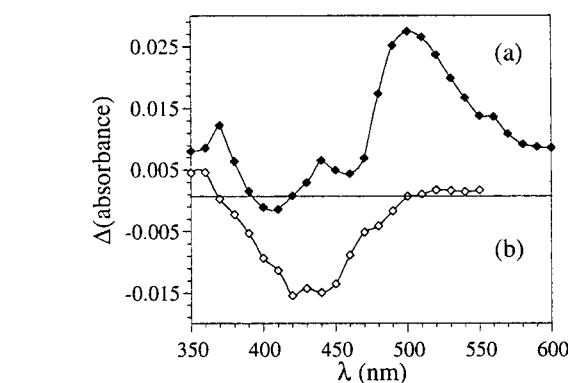


**Figure 8.** (a) (solid diamond) Transient differential absorption spectrum for the system  $[\text{Ru}(\text{TAP})_2\text{Phen}]^{2+} + \text{Nmet-quinoline}$  ( $10^{-2}$  M) in acetonitrile, 3  $\mu\text{s}$  after the laser pulse at 400 nm. (b) (open diamond) Transient differential absorption spectrum for  $[\text{Ru}(\text{TAP})_2\text{POQ-Nmet}]^{2+}$  in acetonitrile, 3  $\mu\text{s}$  after the laser pulse at 400 nm.

(TAP)<sub>2</sub>acPhen]<sup>2+</sup>, and to 17 ns at pH 9 as compared to those for 740 ns observed for excited  $[\text{Ru}(\text{TAP})_2\text{acPhen}]^{2+}$ .

In order to test the possible influence of the phosphate buffer concentration (which has a  $\text{p}K_a = 7.2$ ) on the luminescence decays of  $[\text{Ru}(\text{TAP})_2\text{POQ-Nmet}]^{2+}$ , measurements have been performed with different buffer concentrations, at constant pH, below and above the buffer  $\text{p}K_a$  (i.e., at pH = 4.5, 6, 6.25, 6.5, 7, 8, and 9). In the pH range 6–7 the decays are biexponential. The long lifetime shortens at higher buffer concentrations, and the preexponential factors remain constant. Outside this pH range, the decays remain single exponentials. In contrast, in the presence of tris buffer (which has a  $\text{p}K_a = 8$ ) and at pH 6.5 and 7, the decays are always biexponential and do not change with buffer concentration. Moreover,  $\tau_{\text{long}}$  is identical to the lifetime of excited  $[\text{Ru}(\text{TAP})_2\text{acPhen}]^{2+}$ .

**Existence of an Intramolecular Electron Transfer in Excited  $[\text{Ru}(\text{TAP})_2\text{POQ-Nmet}]^{2+}$  As Studied by Laser Flash Photolysis.** The laser flash photolysis of  $[\text{Ru}(\text{BPY})_2\text{Phen}]^{2+}$  or  $[\text{Ru}(\text{TAP})_2\text{Phen}]^{2+}$  in MeCN produces a transient differential absorption spectrum, which corresponds to the depletion of the complex, with a recovery time equal to the luminescence lifetime. The same behavior is observed for the system “ $[\text{Ru}(\text{BPY})_2\text{Phen}]^{2+} + \text{Nmet-quinoline}$ ” (Figure 1) and for  $[\text{Ru}(\text{BPY})_2\text{POQ-Nmet}]^{2+}$ . It is concluded that neither an intermolecular nor an intramolecular electron transfer takes place respectively from Nmet-quinoline or from the quinoline unit of the bifunctional compound to the excited  $\text{Ru}(\text{BPY})_2^{2+}$  moiety.

The behavior is rather different for  $[\text{Ru}(\text{TAP})_2\text{Phen}]^{2+} + \text{Nmet-quinoline}$  in an organic solvent or in aqueous solution. The Stern–Volmer plots derived from luminescence lifetimes in DMSO and acetonitrile lead to quenching rate constants by nonprotonated Nmet-quinoline of  $4.7 \times 10^7$  and  $4.7 \times 10^8$   $\text{M}^{-1} \text{s}^{-1}$ , respectively (Table 5). In aqueous solution,  $k_q$  reaches  $1.5 \times 10^9$   $\text{M}^{-1} \text{s}^{-1}$  at pH 9.1 (phosphate buffer, nonprotonated quinoline). No quenching is observed at pH 4.5 when the Nmet-quinoline is protonated. The laser flash photolysis of  $[\text{Ru}(\text{TAP})_2\text{Phen}]^{2+} + \text{Nmet-quinoline}$  ( $10^{-2}$  M) in acetonitrile (Figure 8a) leads to a transient differential absorption spectrum

**TABLE 5**

		H <sub>2</sub> O (pH 9.1)	CH <sub>3</sub> OH	CH <sub>3</sub> CN	(CH <sub>3</sub> ) <sub>2</sub> CO	DMSO	DMF	H <sub>2</sub> O (pH 4.5)
$k_{\text{intra}}$ ( $10^6 \text{ s}^{-1}$ ) <sup>a</sup>	air	50	18	7.6	5.3	2.4	2.2	0
	Ar		16	8.3	4.6	2.5	2.2	
$k_q$ ( $10^7 \text{ s}^{-1} \text{ M}^{-1}$ ) <sup>b</sup>	air	150		47		4.7		0

<sup>a</sup>  $k_{\text{intra}}$ : intramolecular luminescence quenching rate constants (in  $\text{s}^{-1}$ ) for  $[\text{Ru}(\text{TAP})_2\text{POQ-Nmet}]^{2+}$  calculated from  $k_{\text{intra}} = \tau_{\text{short}}^{-1} - \tau_{\text{ref}}^{-1}$  (see text). <sup>b</sup>  $k_q$ : bimolecular quenching rate constants (in  $\text{M}^{-1} \text{s}^{-1}$ ) for  $[\text{Ru}(\text{TAP})_2\text{Phen}]^{2+} + \text{Nmet-quinoline}$ , as determined from Stern–Volmer plots of luminescence lifetimes.

**TABLE 6: Concentration of Reduced Methylviologen  $MV^{+}$  <sup>a</sup>**

complex	$[MV^{2+}]$ (M)	$[MV^{+}]$ (M)
$[Ru(TAP)_2POQ-Nmet]^{2+}$	0.10	$4 \times 10^{-7}$
$[Ru(TAP)_2POQ-Nmet]^{2+}$	0.01	$8 \times 10^{-8}$
$[Ru(TAP)_2Phen]^{2+} + Nmet-quinoline$	0.10	$2 \times 10^{-7}$
$[Ru(TAP)_2Phen]^{2+} + Nmet-quinoline$	0.01	$4 \times 10^{-8}$

<sup>a</sup>  $MV^{+}$  after a laser pulse of (i)  $[Ru(TAP)_2POQ-Nmet]^{2+}$  and (ii)  $[Ru(TAP)_2Phen]^{2+} + Nmet-quinoline$  ( $3 \times 10^{-5}$  M), both in the presence of  $MV^{2+}$  in the same experimental conditions, in phosphate buffer at pH 8;  $\epsilon(MV^{+})_{396nm} = 4.2 \times 10^4 \text{ M}^{-1} \text{ cm}^{-1}$  [complex] =  $3 \times 10^{-5}$  M; excitation at 400 nm.

characteristic of the monoreduced species  $[Ru(TAP)^-(TAP)-Phen]^{1+}$ ,<sup>43</sup> which disappears in a timescale of a few hundreds microseconds via a bimolecular process. These observations indicate the occurrence of an intermolecular photoelectron transfer from Nmet–quinoline to excited  $[Ru(TAP)_2Phen]^{2+}$ .

For  $[Ru(TAP)_2POQ-Nmet]^{2+}$  in acetonitrile, a very weak transient absorption is observed at 510–550 nm (Figure 8b) and disappears within a longer timescale than the luminescence lifetime of this bifunctional complex. The intensity of the signal is much too weak to allow a kinetic analysis (see Figure 8b). This indicates nevertheless the presence of small amounts of monoreduced metallic unit. The question which is raised is whether this species is formed from an intra- or intermolecular charge transfer process.<sup>44</sup> Indeed, a comparably weak transient absorption is observed from an intermolecular process for the equimolar system  $[Ru(TAP)_2Phen]^{2+} + Nmet-quinoline$  ( $3 \times 10^{-5}$  M), where the concentration of added quencher is equivalent to the concentration of the bifunctional complex in the previous experiment. Therefore the weak transient absorption observed for the bifunctional complex (Figure 8b) (at a concentration of  $3 \times 10^{-5}$  M) could also originate from an intermolecular quenching of the excited metallic unit of one molecule by an organic unit of another molecule. Therefore the transient for the bifunctional complex in acetonitrile does not necessarily originate from an intramolecular electron transfer.

To probe a possible intramolecular process, the following experiment has been performed. Methylviologen ( $MV^{2+}$ ) at high concentration (Table 6) has been added to an aqueous solution of  $3 \times 10^{-5}$  M  $[Ru(TAP)_2POQ-Nmet]^{2+}$  on one hand and to the system  $[Ru(TAP)_2Phen]^{2+}$  with Nmet–quinoline ( $3 \times 10^{-5}$  M) on the other hand.  $MV^{2+}$  can reoxidize the transient reduced complex unit formed from an intra- and intermolecular process and produce reduced methylviologen ( $MV^{+}$ ) detected at 396 nm ( $\epsilon = 42\,000 \text{ M}^{-1} \text{ cm}^{-1}$ )<sup>45</sup> and 615 nm. The amount of detected  $MV^{+}$  reflects thus the amount of reduced complex which originates from both processes. As shown in Table 6, the amount of  $MV^{+}$  formed with the bifunctional complex is approximately twice as large as that produced with the system  $[Ru(TAP)_2Phen]^{2+}$  with Nmet–quinoline ( $3 \times 10^{-5}$  M). This thus suggests that for the bifunctional  $[Ru(TAP)_2POQ-Nmet]^{2+}$  both inter- and intramolecular electron transfer processes do occur.<sup>46</sup>

## Discussion

**Comparison between the BPY and TAP Complexes.** The difference in properties between these two types of complexes originates mainly from the difference in the level of the BPY and TAP  $\pi^*$  orbitals. The TAP  $\pi^*$  orbital is much lower or more stabilized in energy than that of the BPY or POQ ligand.<sup>20</sup> This leads to two main consequences: (i) the TAP complexes in the excited state are highly oxidizing which induces an electron transfer (inter- or intramolecular)<sup>43</sup> from a donor, (ii)

the luminophore of lower energy changes from a Ru to BPY or to POQ CT transition (e.g.,  $[Ru(BPY)_2POQ-Nmet]^{2+}$ ) into a Ru to TAP CT transition (e.g.,  $[Ru(TAP)_2POQ-Nmet]^{2+}$ ). These two points are illustrated with the mono- and bifunctional complexes respectively.

**Monofunctional Complexes.** The luminescence properties of  $[Ru(TAP)_2acPhen]^{2+}$  are identical to those of the nonfunctionalized complex (i.e.,  $[Ru(TAP)_2Phen]^{2+}$ ). This is attributed to the fact that the same luminophore at lower energy, thus the  $[Ru-TAP]$  CT state, controls these properties. This is not the case for the BPY complexes where the luminescence characteristics are controlled by CT transitions<sup>47,48</sup> including slightly different ligands (i.e., acPhen and Phen).

The difference in the photoredox properties of the BPY and TAP complexes is also clearly illustrated. Indeed the addition of the Nmet–quinoline molecule to the solution, and when it is nonprotonated, produces a luminescence quenching of the TAP compound (due to an intermolecular electron transfer, see below). This is not the case for the corresponding BPY complex. However, when the Nmet–quinoline donor is protonated at pH 4.5, quenching of emission of the TAP complex does not take place. This is probably due to the insufficient reducing power of the protonated Nmet–quinoline as compared to the nonprotonated species, so that quenching by electron transfer (see below) is no longer thermodynamically feasible.

**Bifunctional Complexes.** For the bifunctional BPY complex, independent of the degree of protonation of the aminoquinoline unit, the excited state lifetime is always comparable to that of  $[Ru(BPY)_2acPhen]^{2+}$  which indicates an absence of intramolecular quenching in the bifunctional compound. The substitution of the BPY by TAP ligands in the bifunctional complex induces a shortening of the luminescence lifetime which is attributed to intramolecular quenching. In this case, too, when the quinoline unit is protonated, the intramolecular quenching disappears, as indicated by the long luminescence lifetime which approaches that of excited  $[Ru(TAP)_2acPhen]^{2+}$  and  $[Ru(TAP)_2Phen]^{2+}$  in acidic medium. This absence of quenching could also be attributed to an electrostatic repulsion between the two charged subunits, favoring the unfolded form and thus preventing efficient quenching.

**Two Emitting Species in  $[Ru(TAP)_2POQ-Nmet]^{2+}$ . Presence of an Intramolecular Photoelectron Transfer.** Both emission components of the bifunctional complex  $[Ru(TAP)_2POQ-Nmet]^{2+}$  originate from the metallic unit which in one case bears a protonated and in the other case a nonprotonated quinoline unit. In an organic solvent (MeCN, Figure 5), using pulsed irradiation, these two species are distinguished by their luminescence decays. Indeed, the correlation between the contribution of each decay component with the degree of protonation of the quinoline unit (caused by addition of methanesulphonic acid) clearly exhibits that the longer lifetime is associated with the protonated species, whereas the shorter is associated with the nonprotonated species. These two species are in slow equilibrium as compared to the excited state lifetime of the luminescing complex in organic solvent. The shorter lifetime can be attributed to an intramolecular quenching by the nonprotonated quinoline unit. The single-exponential character of this short component which occurs in the presence of a base leads to the conclusion that all the conformers (all the degrees of folding) are in fast equilibrium as compared to the deactivation rate to the ground state (i.e.,  $\gg 1.4 \times 10^6 \text{ s}^{-1}$ ).<sup>37,49–52</sup>

In aqueous solution, the pH dependence of the relative emission intensity of excited  $[Ru(TAP)_2POQ-Nmet]^{2+}$  (Figure 6b), which is comparable to the pH dependence of the absorption

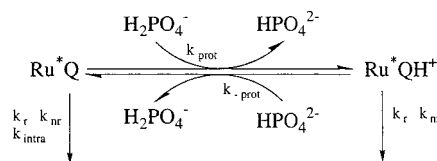
at 354 nm of the quinoline unit (Figure 4), confirms that also in water, (i) there are two species (protonated/nonprotonated) in equilibrium and (ii) the intramolecular luminescence quenching appears only for the nonprotonated quinoline unit. The effect of buffers on the equilibrium of the two excited species is discussed in the annexe.

In water or in organic solvent, the question which has to be raised concerns the origin of the intramolecular quenching. Flash photolysis experiments demonstrate that a photo-induced *intermolecular* electron transfer definitely takes place between the separated moieties (monofunctional complex  $[\text{Ru}(\text{TAP})_2\text{Phen}]^{2+}$  and the Nmet-quinoline quencher). By extrapolation they suggest that this process could be at the origin of the *intramolecular* quenching between the linked units. Thermodynamic data indicate indeed that the process can take place. With a reduction potential of the excited metallic unit estimated to be +1.13 V/SCE<sup>28</sup> (compared to +0.66 V/SCE for the equivalent BPY metallic unit<sup>3</sup>) and the oxidation potential of the Nmet-quinoline unit of  $\approx +1.32$  V/SCE<sup>28</sup>, the free energy change corresponds to  $\approx +0.19$  eV. The absence of important transient absorption displaying the characteristics of the  $\text{TAP}^{*+}$  chromophore for the experiment in acetonitrile with  $[\text{Ru}(\text{TAP})_2\text{POQ-Nmet}]^{2+}$ , in the time scale of hundreds nanoseconds, does not necessarily indicate an absence of intramolecular charge transfer process. The intramolecular electron transfer could indeed be followed by a fast back electron transfer. The data in Table 6 for aqueous solutions confirm that methylviologen scavenges a reduced transient which originates from such an intramolecular charge transfer. This process results in the formation of only small concentrations of  $\text{MV}^{*+}$  despite the high concentration ( $10^{-1}$  M) and the high reduction rate of  $\text{MV}^{2+}$  ( $k_{\text{reduction}} \approx 10^{10} \text{ M}^{-1} \text{ s}^{-1} \times 0.1 \text{ M} = 10^9 \text{ s}^{-1}$ ). Moreover, as no  $\text{MV}^{*+}$  could be detected with a concentration of  $\text{MV}^{2+}$  below  $10^{-2}$  M (Table 6), the rate constant of the competing intramolecular back electron transfer should be  $\gg 10^8$ – $10^9 \text{ s}^{-1}$ . This leads to the conclusion that in the absence of  $\text{MV}^{2+}$  the monoreduced  $\text{Ru}(\text{TAP}^{*+})(\text{TAP})^{1+}$  moiety has a short lifetime ( $\ll 1$ – $10$  ns), and therefore cannot be detected with our flash photolysis equipment (see Experimental Section).

As the different conformers (with different degrees of folding) are in fast equilibrium they have probably different intramolecular electron transfer rate constants. Therefore an average rate constant ( $k_{\text{intra}}$ ) could be estimated for the intramolecular quenching in the different solvents.

The inverse of the lifetime of the nonprotonated excited  $[\text{Ru}(\text{TAP})_2\text{POQ-Nmet}]^{2+}$  in a series of solvents is given by  $\tau_{\text{short}}^{-1} = k_r + k_{\text{nr}} + k_{\text{intra}}$ , where  $k_r + k_{\text{nr}} = \tau_{\text{ref}}^{-1}$  corresponds to the emission lifetime of the monofunctional reference complex in the corresponding solvent. Thus  $k_{\text{intra}}$  corresponds to  $\tau_{\text{short}}^{-1} - \tau_{\text{ref}}^{-1}$  (Table 5)<sup>49,51,53</sup> and follows the sequence:  $k_{\text{intra}}$  in  $\text{H}_2\text{O}$  (pH 9.1) >  $\text{CH}_3\text{CN}$  >  $\text{DMSO}$ . It turns out that the intermolecular quenching rate constants ( $k_q$ ) (Table 5) follows the same sequence:  $k_q$  in  $\text{H}_2\text{O}$  (pH 9.1) >  $\text{CH}_3\text{CN}$  >  $\text{DMSO}$ . As  $k_q$  in the organic solvents is smaller than the rate constant of diffusion,  $k_q$  is then given by  $k_q = K_{\text{diff}}k_{\text{et}}$  ( $K_{\text{diff}}$  = the equilibrium constant for the diffusion and  $k_{\text{et}}$  = the rate constant for the electron transfer).<sup>54–56</sup> Therefore, if the diffusion equilibrium does not vary significantly with the solvent,<sup>57</sup> and because the electron transfer is more efficient in aqueous solution than in organic solvent,  $k_{\text{et}}$  intermolecular follows the same sequence as the intramolecular electron transfer. This conclusion supplies a supplementary argument in favor of an intramolecular luminescence quenching by charge transfer in excited  $[\text{Ru}(\text{TAP})_2\text{POQ-Nmet}]^{2+}$ .

## SCHEME 1



<sup>a</sup>  $k_r$  and  $k_{\text{nr}}$ : radiative and nonradiative deactivation rate constants.  $k_{\text{prot}}$  and  $k_{\text{prot-}}$ : protonation–deprotonation rate constants.  $k_{\text{intra}}$ : intramolecular quenching rate constant.  $[\text{Ru}^*\text{Q}]$ : concentration of nonprotonated species.  $[\text{Ru}^*\text{QH}^+]$ : concentration of protonated species.

**Annexe: Kinetic Treatment of the Luminescence Decays of  $[\text{Ru}(\text{TAP})_2\text{POQ-Nmet}]^{2+}$  in Aqueous Solution. Effect of Buffers.** Although the behaviors in organic solvents and in water have similar characteristics, there are important differences which are discussed in this section. First of all, in aqueous solution, the protonated and nonprotonated species are in fast acid–base equilibrium, in the timescale of the luminescence lifetimes. Moreover, these lifetimes are affected by the concentration of the buffer, the percentages of its acid and base form and the nature of the buffer. This suggests that this acid–base equilibrium is mediated by the buffer as illustrated in Scheme 1. The buffer plays a role in the protonation and deprotonation processes, especially in the pH range where the concentrations of  $\text{H}^+$  and  $\text{OH}^-$  are low.

The differential equations for Scheme 1 are

$$\frac{d[\text{Ru}^*\text{Q}](t)}{dt} = -(k_{\text{intra}} + k_r + k_{\text{nr}} + k_{\text{prot}}[\text{H}_2\text{PO}_4^-])[\text{Ru}^*\text{Q}](t) + k_{\text{prot-}}[\text{HPO}_4^{2-}][\text{Ru}^*\text{QH}^+](t) \quad (1)$$

$$\frac{d[\text{Ru}^*\text{QH}^+](t)}{dt} = k_{\text{prot}}[\text{H}_2\text{PO}_4^-][\text{Ru}^*\text{Q}](t) - (k_r + k_{\text{nr}} + k_{\text{prot-}}[\text{HPO}_4^{2-}])[\text{Ru}^*\text{QH}^+](t)$$

This system of equations, where it is assumed that the equilibrium constant of protonation–deprotonation of the quinoline unit is the same in the ground and in the excited state of the metal unit, can be solved analytically and gives two apparent luminescence lifetimes<sup>37</sup> (eq 2)

$$\tau_{\text{short}(+) \text{ or long}(-)} = \frac{2}{k_{\text{intra}} + 2(k_r + k_{\text{nr}}) + k_{\text{prot}}[\text{H}_2\text{PO}_4^-] - k_{\text{prot-}}[\text{HPO}_4^{2-}] \pm \sqrt{R}} \quad (2)$$

$$R = (k_{\text{intra}} + k_{\text{prot}}[\text{H}_2\text{PO}_4^-] - k_{\text{prot-}}[\text{HPO}_4^{2-}])^2 + 4k_{\text{prot}}[\text{H}_2\text{PO}_4^-]k_{\text{prot-}}[\text{HPO}_4^{2-}]$$

Thus biphasic luminescence decays with two apparent lifetimes should be observed, which is indeed the case. We have tried to evaluate the protonation and deprotonation rate constants ( $k_{\text{prot}}$  and  $k_{\text{prot-}}$ ) from the fitting of one of these two apparent luminescence lifetimes ( $\tau_{\text{long}}$ ) (eq 2) versus the concentration of the basic form of the buffer (Figure 9). For these calculations, we assume (1)  $k_r + k_{\text{nr}} = 1/\tau_{\text{T2acPh}}$  ( $\tau_{\text{T2acPh}}$  = luminescence lifetime of  $[\text{Ru}(\text{TAP})_2\text{acPh}]^{2+}$  at the different pH and buffer concentrations which are used), (2)  $k_{\text{intra}} = 1/\tau_{\text{T2POQNmet}} - 1/\tau_{\text{T2acPh}}$  (in the same pH and buffer conditions), (3) the acidic form of the buffer is related to its basic form by



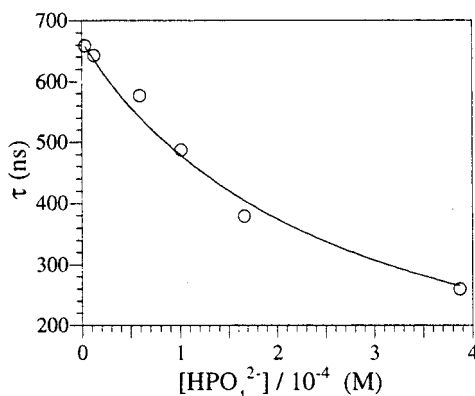


**Figure 9.** Long luminescence lifetimes of  $[\text{Ru}(\text{TAP})_2\text{POQ}-\text{Nmet}]^{2+}$  versus  $[\text{HPO}_4^{2-}]$  (1 mM phosphate buffer; pH, 4.7, 5.3, 6, 6.25, 6.5, and 7), fitted by eq 2.

$$[\text{H}_2\text{PO}_4^{2-}] = [\text{HPO}_4^{2-}] 10^{\text{p}K_{\text{a}}(\text{B})-\text{pH}}$$

$$[\text{HPO}_4^{2-}] + [\text{H}_2\text{PO}_4^{2-}] = [\text{B}] \quad (\text{B} = \text{buffer})$$

(4)  $k_{\text{prot}}$  and  $k_{-\text{prot}}$  are related by

$$k_{\text{prot}} = k_{-\text{prot}} 10^{\text{p}K_{\text{a}}(\text{Q})-\text{p}K_{\text{a}}(\text{B})} \quad (\text{Q} = \text{quinoline})$$

and (5) for the fitting procedure, one parameter has to be adjusted, either  $k_{\text{prot}}$  or  $k_{-\text{prot}}$ . The fitting leads to a value of  $6 \times 10^9 \text{ M}^{-1} \text{ s}^{-1}$  for  $k_{-\text{prot}}$  and  $4 \times 10^8 \text{ M}^{-1} \text{ s}^{-1}$  for  $k_{\text{prot}}$ .

On the other hand, the concentrations of  $[\text{Ru}^*\text{Q}] + [\text{Ru}^*\text{QH}^+]$  can also be calculated as a function of time by numerical solutions of eq 1. These calculations are based on Markov chains, and include the same five assumptions as those outlined above. Under those conditions, the calculated decays of  $\text{Ru}^*\text{Q}$  and  $\text{Ru}^*\text{QH}^+$  are biexponential. Moreover, the values found for the corresponding time constants are equal to the lifetimes determined experimentally if  $k_{\text{prot}}$  and  $k_{-\text{prot}}$  have the values of  $4 \times 10^8 \text{ M}^{-1} \text{ s}^{-1}$  and  $6 \times 10^9 \text{ M}^{-1} \text{ s}^{-1}$  respectively (i.e., the same as those obtained from the analytical solution of eq 2). In accord with experimental observations, the preexponential factors of the calculated biexponential functions correspond to the percentages of  $\text{Ru}^*\text{Q}$  and  $\text{Ru}^*\text{QH}^+$  at time zero, as calculated from the acid–base equilibrium constant in the ground state ( $[\text{RuQ}] = [\text{RuQH}^+] 10^{\text{pH}-\text{p}K_{\text{a}}(\text{Q})}$ ;  $[\text{RuQ}] + [\text{RuQH}^+] = [\text{complex}]$ ).

The buffer dependence at intermediate pH, can also be explained by this scheme. At pH between 5 and 7, the quinoline unit in  $[\text{Ru}(\text{TAP})_2\text{POQ}-\text{Nmet}]^{2+}$  ( $\text{p}K_{\text{a}} = 6.1$ ) is present as both the protonated and nonprotonated forms, which are in equilibrium during the excited state lifetime of the metallic unit. The two observed lifetimes in that case correspond to the two apparent lifetimes of eq 2. As observed experimentally, by increasing the pH from 5 to 7, the longer lifetime (starting at pH 5 with a value close to that of excited  $[\text{Ru}(\text{TAP})_2\text{acPhen}]^{2+}$ ) shortens. This corresponds to the increase in concentration of the basic form of the phosphate buffer ( $\text{p}K_{\text{a}} = 7.2$ ), which accelerates the rate of deprotonation [ $(k_{-\text{prot}}[\text{base}])$  changes from  $0.4 \times 10^6 \text{ s}^{-1}$  at pH 6 to  $4 \times 10^6 \text{ s}^{-1}$  at pH 7]. The deprotonation thus competes with the deactivation pathways of the excited metallic unit ( $1.5 \times 10^6 \text{ s}^{-1}$ ). Therefore at a constant pH (range 6–7, phosphate buffer), an increase of the buffer concentration induces a faster acid–base equilibrium, which leads to a shortening of the longer apparent lifetime. On the other hand, when the phosphate buffer is replaced by tris buffer ( $\text{p}K_{\text{a}} = 8$ ), an increase of pH from 6 to 7 does not correspond to a sufficiently important increase in the basic form of the buffer to induce a change in the deprotonation rate of  $\text{Ru}^*\text{QH}^+$ .

Therefore, with tris buffer a fast acid–base equilibrium is not established during the excited state lifetime of the metallic unit so that the situation is similar to that in organic solvents.

## Conclusion

The complete photophysical mechanism presented in this paper facilitates the exploitation of these results for the design of new “light switches” in the presence of DNA.

The bifunctional complex  $[\text{Ru}(\text{TAP})_2\text{POQ}-\text{Nmet}]^{2+}$ , described in this work, has a low-emission quantum yield in water because of the intramolecular quenching process by intramolecular charge transfer. It has been observed that the luminescence is restored upon interaction with some polynucleotides.<sup>58</sup> Indeed the polynucleotide induces (i) protonation of the quinoline moiety<sup>59,60</sup>, which makes this unit less reducing, and (ii) unfolding of the molecule as also observed by Schanze et al.<sup>61</sup> for other complexes. To increase the efficiency of the  $\text{Ru}(\text{II})$  bifunctional complex as a DNA photoprobe, the intramolecular luminescence quenching in water should be further increased. This can be done by increasing the driving force of the intramolecular electron transfer. On the other hand, as the excited  $\text{Ru}(\text{TAP})_2^{2+}$  unit is capable of abstracting an electron from the guanine sites of DNA, the bifunctional complex should also present a potential interest as a photoreagent with DNA as demonstrated with monofunctional complexes.<sup>14</sup>

**Acknowledgment.** The authors thank J. P. Lecomte for helpful discussions. A.D.G. and A.K.D. are grateful to the Communauté Française de Belgique, Direction Générale de l’Enseignement Supérieur et de la Recherche (Grant ARC 91/6-149) and to the SSTC (PAI-IUAP 4/11 program) for financial support of this work. We also thank J. Kelly from the Trinity College Dublin and G. Orellana from the Universidad Complutense de Madrid who allowed A.D.G. to perform single-photon counting measurements in their laboratory thanks to the support of a European Communities Human Capital and Mobility Programme (Dublin). We are also grateful to A. Van Dorsselaer (University of Strasbourg, France) for the ESMS data. A.D.G. has been supported by I.R.S.I.A. and by a research training grant from the Luxembourg Ministry of Education and Vocational Training, as Boursier de l’ULB.

**Supporting Information Available:** ESMS isotopic distribution for  $[\text{Ru}(\text{TAP})_2\text{POQ}-\text{Nmet}]^{2+}$  (1 page). Ordering information is given on any current masthead page.

## References and Notes

- Balzani, V.; Barigelli, F.; De Cola, L. In *Topics in Current Chemistry*; Heidelberg, S. V. G., Ed.; Springer Verlag: Berlin, 1990; Vol. 158, pp 31–71.
- Juris, A.; Balzani, V.; Barigelli, F.; Campagna, S.; Belser, P.; von Zelewsky, A. *Coord. Chem. Rev.* **1988**, *84*, 85.
- Kalyanasundaram, K. *Coord. Chem. Rev.* **1982**, *46*, 159.
- Meyer, T. J. *Acc. Chem. Res.* **1989**, *22*, 163.
- Norris, J. R., Jr.; Meiseld, D., Eds. *Photochemical Energy Conversion*, Proceedings of the 7th International Conference on Photochemical Conversion and Storage of Solar Energy, Evanston, IL, July 31–Aug 5, 1988; Elsevier: New York, 1988.
- Karlsson, K.; Kirsch-De Mesmaeker, A. *J. Phys. Chem.* **1991**, *95*, 10681.
- Lin, C. T.; Sutin, N. *J. Phys. Chem.* **1976**, *80*, 97.
- Mecklenburg, S. L.; Peek, B. M.; Schoonover, J. R.; McCafferty, D. G.; Wall, C. G.; Erickson, B. W.; Meyer, T. J. *J. Am. Chem. Soc.* **1993**, *115*, 5479.
- Davidson, R. S.; Hilchenbach, M. M. *J. Photochem. Photobiol., B* **1992**, *52*, 431.
- Barton, J. K.; Basile, L. A.; Danishefsky, A.; Alexandrescu, A. *Proc. Natl. Acad. Sci. U.S.A.* **1984**, *81*, 1961.
- Wells, R. D. *J. Biol. Chem.* **1988**, *263*, 1095.
- Gough, G. W.; Lilley, D. M. *Nature* **1985**, *313*, 154.

- (13) Chow, C. S.; Barton, J. K. In *Methods in Enzymology*; Academic Press, Inc.: New York, 1992; Vol. 212, pp 219–242.
- (14) Lecomte, J.-P.; Kirsch-De Mesmaeker, A.; Feeney, M. M.; Kelly, J. M. *Inorg. Chem.* **1995**, *34*, 6481.
- (15) Kirsch-De Mesmaeker, A.; Orellana, G.; Barton, J. K.; Turro, N. *J. Photochem. Photobiol.* **1990**, *52*, 461.
- (16) Kelly, J. M.; McConnell, D. J.; OhUigin, C.; Tossi, A. B.; Kirsch-De Mesmaeker, A.; Masschelein, A.; Nasielski, J. *J. Chem. Soc., Chem. Commun.* **1987**, 1821.
- (17) Kelly, J. M.; Feeney, M. M.; Tossi, A. B.; Lecomte, J.-P.; Kirsch-De Mesmaeker, A. *Anti-Cancer Drug Des.* **1990**, *5*, 69.
- (18) Feeney, M. M.; Kelly, J. M.; Tossi, A. B.; Kirsch-De Mesmaeker, A.; Lecomte, J.-P. *J. Photochem. Photobiol., B* **1994**, *23*, 69.
- (19) Kirsch-De Mesmaeker, A.; Nasielski-Hinkens, R.; Maetens, D.; Pauwels, D.; Nasielski, J. *Inorg. Chem.* **1984**, *23*, 377.
- (20) Masschelein, A.; Jacquet, L.; Kirsch-De Mesmaeker, A.; Nasielski, J. *Inorg. Chem.* **1990**, *29*, 855.
- (21) Jacquet, L.; Kirsch-De Mesmaeker, A. *J. Chem. Soc., Faraday Trans.* **1992**, *88*, 2471.
- (22) Lecomte, J.-P.; Kirsch-De Mesmaeker, A.; Kelly, J. M.; Tossi, A. B.; Görner, H. *Photochem. Photobiol.* **1992**, *55*, 681.
- (23) Tossi, A. B.; Kelly, J. M. *Photochem. Photobiol.* **1989**, *49*, 545.
- (24) Jacquet, L.; Kelly, J. M.; Kirsch-De Mesmaeker, A. *J. Chem. Soc., Chem. Commun.* **1995**, *9*, 913.
- (25) Dervan, P. B. *Science* **1986**, *232*, 464.
- (26) Strobel, S. A.; Doucette-Stamm, L. A.; Riba, L.; Housman, D. E.; Dervan, P. B. *Nature* **1991**, *254*, 1639.
- (27) Kelly, J. M.; Tossi, A. B.; McConnell, D. J.; OhUigin, C. *Nucleic Acids Res.* **1985**, *13*, 6017.
- (28) Lecomte, J.-P.; Kirsch-De Mesmaeker, A.; Demeunynck, M.; Lhomme, J. *J. Chem. Soc., Faraday Trans.* **1993**, *89*, 3261.
- (29) Bolte, J.; Demeunck, C.; Lhomme, J.; Fourmié-Zaluski, M.; Roques, B. *Biochemistry* **1979**, *18*, 4928.
- (30) Bolte, J.; Demeunck, C.; Lhomme, M. F.; Lhomme, J.; Barbet, J.; Roques, B. *J. Am. Chem. Soc.* **1982**, *104*, 760.
- (31) Sullivan, B.; Salmon, D.; Meyer, T. J. *Inorg. Chem.* **1982**, *21*, 3334.
- (32) Baggot, J. E.; Gregory, G. K.; Pilling, M. J.; Andreson, S.; Seddon, K. R.; Turp, J. E. *J. Chem. Soc., Faraday Trans.* **1983**, *79*, 195.
- (33) Del Guerzo, A.; Kirsch-De Mesmaeker, A. Results to be published.
- (34) By HPLC it is difficult to detect the presence of bifunctional complexes which would originate from (photo)decomposition of  $[\text{Ru}(\text{TAP})_2\text{POQ}-\text{Nmet}]^{2+}$ . However, under pulsed excitation, the luminescence decay in MeCN with an excess of piperidine is disturbed by a slight contribution of an impurity. This species has the same characteristics as the monofunctional complex. Upon analysis of the relative emission quantum yields in basic solution, this impurity can be estimated as <2%. Similar problems with other derivatized complexes have been reported.<sup>49,51,53</sup>
- (35) Lin, C. T.; Boettcher, W.; Chou, M.; Creutz, C.; Sutin, N. *J. Am. Chem. Soc.* **1976**, *98*, 6536.
- (36) Bevington, P. R. *Data Reduction and Errors Analysis for the Physical Sciences*; McGraw Hill: New York, 1969.
- (37) Demas, J. N. *Excited State Lifetime Measurements*; Academic Press: New York, 1983.
- (38) Ameloot, M.; Boens, N.; Andriessen, R.; Van den Bergh, V.; De Schryver, F. *J. Phys. Chem.* **1991**, *95*, 2041.
- (39) Nord, K.; Karlsen, J.; Tonnesen, H. H. *Photochem. Photobiol.* **1994**, *60*, 427.
- (40) Kirsch-De Mesmaeker, A.; Jacquet, L.; Nasielski, J. *Inorg. Chem.* **1988**, *27*, 4451.
- (41) At constant pH ( $\text{pH} \leq \text{pK}_a + 1$  of the phosphate buffer) and for increasing concentrations of buffer, a decrease of luminescence is observed.<sup>28</sup> Thus, the slight curvature in Figure 6a around pH 5–7 is due to the quenching by the acidic form of the phosphate buffer.<sup>40</sup>
- (42) For this complex, the luminescence quenching rate constant (where the quenching is caused by the acidic form of the phosphate buffer) is determined, at constant pH (6.5), from the lifetimes and is  $1 \times 10^8 \text{ M}^{-1} \text{ s}^{-1}$ .
- (43) Masschelein, A.; Kirsch-De Mesmaeker, A. *New J. Chem.* **1987**, *11*, 329.
- (44) Although no significant change in the luminescence lifetimes of the bifunctional complex is observed when its concentration is increased from  $1.5 \times 10^{-5}$  to  $7 \times 10^{-4} \text{ M}$ , flash photolysis experiments indicate nevertheless that an intermolecular process would take place.
- (45) Watanabe, T.; Honda, K. *J. Phys. Chem.* **1982**, *86*, 2617.
- (46) It should be noted that a bimolecular quenching is less probable with  $[\text{Ru}(\text{TAP})_2\text{POQ}-\text{Nmet}]^{2+}$  ( $3 \times 10^{-5} \text{ M}$ ) than with the system  $[\text{Ru}(\text{TAP})_2\text{Phen}]^{2+} + \text{Nmet}$ -quinoline ( $3 \times 10^{-5} \text{ M}$ ). Indeed, in aqueous solution at pH 8 the luminescence lifetime of the excited  $\text{Ru}(\text{TAP})_2^{2+}$  unit of the bifunctional complex is shorter (17 ns) than that of the complex  $[\text{Ru}(\text{TAP})_2\text{Phen}]^{2+}$  (740 ns) of the reference system in the same conditions. This comment argues more strongly in favor of an intramolecular charge transfer process in the bifunctional complex.
- (47) Kumar, C. V.; Barton, J. K.; Gould, I. R.; Turro, N. J.; Van Houten, J. *Inorg. Chem.* **1988**, *27*, 648.
- (48) Chang, Y. J.; Xu, X.; Yabe, T.; Yu, S.-C.; Angerson, D. R.; Orman, L. K.; Hopkins, J. B. *J. Phys. Chem.* **1990**, *94*, 729.
- (49) Larson, S. L.; Michael Elliott, C.; Kelley, D. F. *Inorg. Chem.* **1996**, *35*, 2070.
- (50) Boyde, S.; Strouse, G. F.; Jones Jr., W. E.; Meyer, T. J. *J. Am. Chem. Soc.* **1989**, *111*, 7448.
- (51) Ryu, C. K.; Wang, R.; Schmehl, R.; Ferrer, S.; Ludwikow, M.; Merkert, J. W.; Headford, C. E. L.; Elliot, C. M. *J. Am. Chem. Soc.* **1992**, *114*, 430.
- (52) Hamachi, I.; Tanaka, S.; Shinkai, S. *J. Am. Chem. Soc.* **1993**, *115*, 10458.
- (53) Schanze, K. S.; Sauer, K. *J. Am. Chem. Soc.* **1988**, *110*, 1180.
- (54) Kavarnos, G. J.; Turro, N. J. *Chem. Rev.* **1986**, *86*, 401.
- (55) Kavarnos, G. J. In *Topics in Current Chemistry*; Heidelberg, S. V. B., Ed.; Springer Verlag: Berlin, 1990; Vol. 156, pp 23–58.
- (56) Balzani, V.; Scandola, F.; Orlandi, G.; Sabatini, N.; Indelli, M. *J. Am. Chem. Soc.* **1981**, *103*, 3370.
- (57) Chiorboli, C.; Scandola, F. *J. Phys. Chem.* **1986**, *90*, 2211.
- (58) Del Guerzo, A.; Kirsch-De Mesmaeker, A. Results to be published.
- (59) Lamm, G.; Pack, G. R. *Biophysics* **1990**, *87*, 9033.
- (60) Pack, G. R.; Wong, L. *Chem. Phys.* **1996**, *204*, 279.
- (61) Thornton, N. B.; Schanze, K. S. *Inorg. Chem.* **1993**, *32*, 4994.